Rapid Communications

Peculiar behavior of Si cluster ions in a high-energy-density solid Al plasma

S. Kawata,[1,*] C. Deutsch,[2] and Y. J. Gu[3,4]

[1]*Graduate School of Engineering, Utsunomiya University, Utsunomiya 321-8585, Japan*
[2]*Laboratoire de Physique des Gaz et des Plasmas (LPGP), Université Paris-Saclay, 91405 Orsay, France*
[3]*Institute of Physics of the ASCR, ELI-Beamlines, Na Slovance 2, 18221 Prague, Czech Republic*
[4]*Institute of Plasma Physics of the CAS, Za Slovankou 1782/3, 18200 Prague, Czech Republic*

(Received 24 August 2018; published 31 January 2019)

Peculiar behavior is found in a Si cluster ion, moving with a speed of $\sim 0.22c$ (c: speed of light) in a solid Al plasma in the context of cluster-ion beam driven inertial confinement fusion: The Si ion, moving closely behind the forward-moving Si ion for a distance of several Å in the cluster, feels the wake field generated by the forward Si. The acceleration interaction force on the rear Si ion by the forward-moving ion may balance with the deceleration backward force in the longitudinal-moving direction. The forward-moving Si ion would be decelerated, as an isolated ion is decelerated without correlation. However, the deceleration of the rear Si ion, moving behind closely, would be reduced significantly. The rear Si ion may catch up and overtake the forward-moving Si ion in the cluster during the Si cluster-ion interaction with the high-density Al plasma. This peculiar behavior appears when the ions are aligned well longitudinally. The wake field is confined around the Si ion in the forward and transverse directions for a distance smaller than the Si cluster interionic distance l_c. However, the tail of the wake field extends beyond l_c due to the Si ion high speed of $\sim 0.22c$. Therefore, the peculiar behavior shown above appears only for the ions in one cluster aligned well longitudinally.

DOI: 10.1103/PhysRevE.99.011201

The interaction of cluster ions with matter has attracted serious attention in numerous scientific areas, including a cluster interaction with intense lasers to induce a Coulomb explosion [1–4], fast clusters' interaction with targets based on recent accelerator technology advances [5,6], and a cluster-ion beam application to an inertial fusion driver. In ion beam inertial fusion applications especially, a preferable ion speed may be about $0.1c$–$0.25c$, that is, around 10–50 Mev/u [7–9]. Instead of the ion beam, cluster-ion beam inertial fusion has been also proposed [10,11]. In cluster-ion beam (CIB) driven inertial fusion (CIF), it is expected to deposit the cluster beam energy in a small volume of the energy absorber of an inertial fusion fuel pellet by a correlated ion stopping enhancement in plasmas [12–18].

In the correlated cluster stopping in a plasma, the Coulomb explosion of the cluster, the vicinage effect on the cluster stopping, and the wake field by the fast cluster have been studied intensively [1–4,12–19]. If the clusters deposit their energy in the material more than the individual ions, the ratio q/A of the charge q and the mass A can be reduced in CIF, and the CIB space-charge effect on the beam transport may be also reduced inside the accelerator and also during the CIB transport [6,20].

In the context of CIF, CIBs interact with a solid material of Al or Au or so, depending on the fuel target design [7,10,11,20]. In this Rapid Communication, Si clusters and a solid Al target are employed to study the detailed behavior of each cluster ion in a high-energy-density classical plasma, in which the electron Fermi degeneracy is solved.

In high-energy-density Al, the Debye shielding length λ_{De} is typically smaller than the Si cluster interionic distance l_c, $\lambda_{De} < l_c$. The wake field is localized around each ion, and does not cover the whole cluster. Even at room temperature, at which the solid Al free electrons are in the Fermi degenerated state, the Fermi shielding length $\lambda_{Fe} \sim \sqrt{E_F/(6\pi n_e e^2)}$ is typically smaller than the Si cluster interionic distance l_c, $\lambda_{Fe} < l_c$. Here, E_F is the Fermi energy. Hereafter, we treat the high-energy-density plasma classically in the context of CIF.

For a fast-moving ion with $v_0 \gg \sqrt{T_e/m_e}$, the wake field, localized in the transverse and forward directions, extends beyond λ_{De}, so that the strong interaction between a couple of ions in one cluster becomes dominant in the high-energy-density plasma. Here, T_e is the electron temperature and m_e the electron mass. Figure 1 shows a schematic diagram of the electric wake field potential, generated by one swift ion in a high-energy-density plasma. In one cluster moving with a high speed of $v_0/\sqrt{T_e/m_e} \gg 1$, a Si ion located behind a forward-moving Si ion may catch up and overtake the forward-moving Si in the cluster during the Si cluster interaction with the high-energy-density Al plasma.

In CIF the solid Al and the fuel target material are heated up to a temperature that is higher than the Fermi temperature typically in a short period of less than a ns by CIB illumination. An ~MJ main driver energy reaches the fuel target after several ns of the foot pulse [7,10,11,20]. The typical interionic distance l_c of a Si cluster is about 5 Å $= 5 \times 10^{-10}$ m. In the high-energy-density solid metal Al, the Si cluster-ion charge is quickly shielded by the Al free electrons, and the Debye shielding length λ_{De} is typically smaller than l_c. After significant heating by the intense CIBs in CIF, the target temperature may become a few hundreds eV [7,10,11]. Even

*kwt@cc.utsunomiya-u.ac.jp

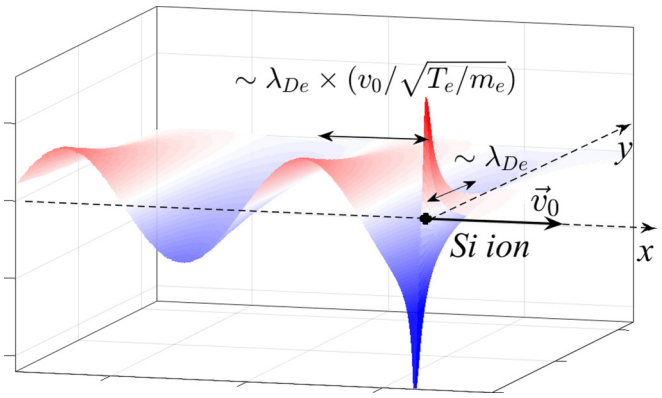

FIG. 1. Schematic diagram of the electric net potential (the wake potential and the potential of the bare Si ion) generated by a swift ion. In high-density solid Al the wake field is localized in the transverse direction and elongated longitudinally behind the Si ion, so that only the Si ion just behind the Si ion in the linearly aligned direction is influenced, $\lambda_{\rm De} < l_c$. Here, l_c is the Si cluster interionic distance. The wake field in the high-energy-density Al covers ions just behind the fast-moving ion.

at an electron high temperature of 100 eV, $\lambda_{\rm De} < l_c$. Here, we found that the vicinage effect is limited to a couple of Si ions moving in parallel to the moving direction among Si cluster ions in the solid high-energy-density Al, and the wake field, generated by one swift Si ion, influences the vicinage Si ion just behind the Si ion involved. While the cluster travels in the solid Al, the Si ion behind the forward-moving precursor Si ion closely catches up and overtakes the precursor Si ion. This intriguing behavior of each Si ion in one cluster is discussed and presented in this Rapid Communication.

On the other hand, the fast single-ion behavior in the high-density plasma has been also studied intensively [21–25]. In a high-temperature dense plasma, assume one fast-moving ion. First, the total electric potential, generated by a swift ion $q\delta(\vec{r} - \vec{v}_0 t)$, is estimated: $\phi_{\rm total} = \phi_{\rm ind} + \phi_{\rm ext}$. Here, $\vec{v}_0$ is the velocity of the ion. In our case, $v_0/\sqrt{T_e/m_e} \gg 1$, and typically $v_0/\sqrt{T_e/m_e} \simeq 5$–$15$. In the linear response framework [25], we can easily describe $\phi_{\rm total}$ in the Fourier space,

$$\phi_{\rm total}(\vec{r}, t) = \frac{q}{(2\pi)^3 4\pi\varepsilon_0} \int_{-\infty}^{\infty} d^3k \frac{1}{k^2} \frac{1}{\epsilon(\vec{k}, \vec{k}\cdot\vec{v}_0)} e^{i\vec{k}\cdot(\vec{r}-\vec{v}_0 t)}. \tag{1}$$

Here, $\epsilon(\vec{k}, \vec{k}\cdot\vec{v}_0)$ is the linear response function of the target plasma electron. The response function would be described as follows,

$$\epsilon(\vec{k}, \vec{k}\cdot\vec{v}_0) = 1 + \left(\frac{k_{\rm De}}{k}\right)^2 W\left(\frac{\vec{k}\cdot\vec{v}_0}{k\sqrt{T_e/m_e}}\right). \tag{2}$$

Here, $W(Z)$ is the W function or the Voigt function, and $W(Z) = \exp(-Z^2)\mathrm{erfc}(-iZ)$. Here, we assume $T_e \gg E_F$ $(= \frac{1}{2}mv_F^2)$, where v_F is the Fermi speed. From $\phi_{\rm total}(\vec{r}, t)$, the induced potential is obtained, $\phi_{\rm ind}(\vec{r}) = \phi_{\rm total}(\vec{r}) - \phi_{\rm ext}(\vec{r})$. At $\vec{r} = \vec{r}_0 + \vec{v}_0 t$, the force acting on the swift ion is obtained by the spatial derivative of $\phi_{\rm ind}(\vec{r})$. Then the stopping power is also obtained in the material.

For the rest ion of $\vec{v}_0 = 0$, $W[(\vec{k}\cdot\vec{v}_0)/(k\sqrt{T_e/m_e})] = 1.0$, and $\phi_{\rm ind}(\vec{r}, 0)$ becomes the static Debye screened potential of $\frac{q}{4\pi\varepsilon_0}\exp(-\frac{r}{\lambda_{\rm De}})$, which is isotropic. When $v_0/\sqrt{T_e/m_e} \gg 1$, Eqs. (1) and (2) may show that the screening length depends on the spatial direction [22,25]. Here, we assume $\vec{v}_0 \parallel x$. For $X = x - v_0 t > 0$, the total electric potential becomes almost the bare Coulomb potential [22,23], $\phi_{\rm total}(x, r \equiv \sqrt{y^2 + z^2} = 0) \sim \frac{q}{4\pi\varepsilon_0}\frac{1}{X}$. For $X = x - v_0 t < 0$, $\phi_{\rm ind}(x, r = 0) = \phi_{\rm total}(x) - \phi_{\rm ext}(0, x) \propto \frac{q}{4\pi\varepsilon_0\lambda_{\rm De}} \sin\frac{(x-v_0 t)/\lambda_{\rm De}}{v_0/\sqrt{T_e/m_e}}$ [22]. The wake field, generated by the swift ion, extends in the $-X$ direction wider than $\lambda_{\rm De}$, depending on $v_0/\sqrt{T_e/m_e}$. In the transverse direction at $\vec{k}\cdot\vec{v}_0 \sim 0$, $W(\frac{\vec{k}\cdot\vec{v}_0}{k\sqrt{T_e/m_e}}) \sim 1$, and the usual Debye screening is retrieved. Therefore, the total electric potential $\phi_{\rm total}$, produced by the swift ion $(v_0/\sqrt{T_e/m_e} \gg 1)$, is anisotropic and is elongated in $-X = -(x - v_0 t)$ in our high-energy-density plasma, as shown schematically in Fig. 1.

In this discussion we assumed nondegenerate electrons. In the context of the inertial fusion [7–11], the ion beam or cluster-ion beam input total energy is the order of MJ, and the input pulse length is the order of ∼10 ns. Therefore, the temperature of the energy-absorber material of the fuel target quickly becomes rather high, for example, a few hundreds eV, $T_e \gg E_F$ [7,8,10,11]. The discussions above would be valid during the interaction time of the body of the input ion beam, except for the very initial period of the driver illumination time. At the initial time, the target energy absorber material, say, Al or Pb or so, would be degenerated. In that case, the electron temperature T_F should be introduced instead of T_e [25–28]. In the previous experiments [18,19], the peculiar ion motion of the position exchange presented in this Rapid Communication was not found.

Figure 2 presents the numerical results of the electric fields (a) E_x and (b) E_y generated by a single Si ion moving in a solid Al with a speed (v_x) of $0.221c$. In Figs. 2(a) and 2(b), we computed the electric fields E_x and E_y by using a particle-in-cell (PIC) code of EPOCH [29,30]. In the PIC simulations the electron behavior is not treated by the dielectric response function, but each electron motion is described by the relativistic equation of motion. In this Rapid Communication, the Al ion density is the solid one, and the electron temperature is set to be 10 eV. The ionization degree of Al is 3 in this case. As shown above, the electric field is confined around the Si ion in the forward direction and also in the transverse direction. At the rear side of the Si ion, that is, $X = x - v_0 t < 0$, the wake field appears behind Si with a long tail. In this case, the Debye shielding length is $\lambda_{\rm De} \sim 1$ Å.

The simulation results confirm the analytical estimation results shown above: The electric field is confined around the Si ion in the forward and transverse directions at a distance smaller than the Si cluster interionic distance $l_c \sim 5$ Å. However, the tail of the wake field extends beyond l_c. Therefore, the vicinage effect of a Si cluster appears only between the fast-moving precursor Si ion and the succeeding Si ion behind, and confined in the longitudinal direction $(\parallel \vec{v}_0)$ in the solid Al.

A perfect vicinage effect on a cluster appears [1,2,12–18] when all or almost all of the ions consisting of the cluster are located inside the wake field area generated by the cluster ions; the size of the wake field area shown in Fig. 1 should be larger than the cluster size so that the cluster ions

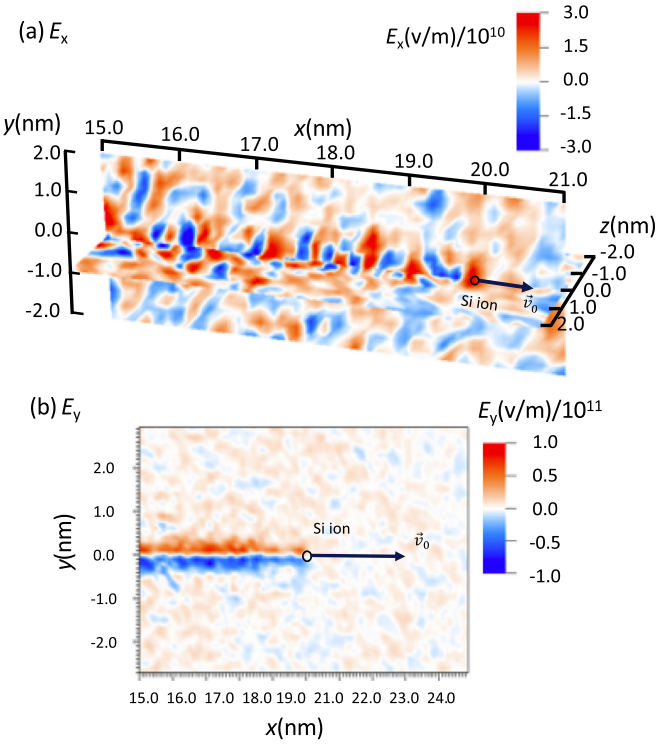

FIG. 2. (a) E_x and (b) E_y generated by a single Si ion moving in a solid Al with a speed (v_x) of $0.221c$.

behave as one accreted huge ion. This is not the case in this work.

Here, let us think about a stopping power of a high-energy-density plasma for a cluster. The stopping power would be described by $-dw/dx = -\sum_j (\vec{v}_j/v_j)\cdot\vec{F}_j$. The summation is carried out over all the ions consisting of the cluster. Here, w is the total cluster-ion energy, and $\vec{F}_j$ the force acting on each ion consisting of the cluster. The total cluster charge density ρ is $\rho = \sum_j \rho_j = \sum_j q_j \delta(\vec{r} - \vec{r}_{j0} - \vec{v}_j t)$. Here, $\vec{r}_{j0}$ is the initial position of the jth ion of the cluster. Here, $\vec{F}_j = q_j\vec{E}(\vec{r}_j) = q_j \sum_i \frac{q_i}{(2\pi)^3\varepsilon_0}\int d^3k \frac{\vec{k}}{k^2}\mathrm{Im}[\frac{1}{\epsilon(\vec{k},\vec{k}\cdot\vec{v}_i)}]\cos(\vec{k}\cdot\vec{r}_{ij})$,

$$-\frac{dw}{dx} = \sum_{ji}\frac{q_j q_i}{(2\pi)^3\varepsilon_0}\int d^3k \frac{\vec{k}\cdot\vec{v}_j}{k^2 v_j}\mathrm{Im}\left[\frac{1}{\epsilon(\vec{k},\vec{k}\cdot\vec{v}_i)}\right] \times \cos(\vec{k}\cdot\vec{r}_{ij}). \quad (3)$$

Here, $\vec{r}_{ji} = \vec{r}_j - \vec{r}_i$. If we can assume $\vec{v}_j \sim \vec{v}_i \sim \vec{v}_0$ (the averaged cluster ion speed), Eq. (3) is simplified to

$$-\frac{dw}{dx} = \frac{1}{(2\pi)^3\varepsilon_0}\int d^3k \frac{\vec{k}\cdot\vec{v}_0}{k^2 v_0}\mathrm{Im}\left[\frac{1}{\epsilon(\vec{k},\vec{k}\cdot\vec{v}_0)}\right] \times \sum_{ji} q_j q_i \cos(\vec{k}\cdot\vec{r}_{ji}). \quad (4)$$

In Eq. (4), $\sum_{ji} q_j q_i \cos(\vec{k}\cdot\vec{r}_{ji}) = \sum_i q_i^2 + \sum_{j\neq i} q_j q_i \cos(\vec{k}\cdot\vec{r}_{ji})$. The second term on the right-hand side in the expression shows the correlation between two of the cluster ions. In previous studies of the vicinage effect on the stopping power for the cluster, this approximation is frequently employed [1,2,12–18]. For the perfect vicinage effect, the stopping power enhancement factor is obtained as $(N + C_2^N)/N = (N + N(N-1)/2)/N = (N+1)/2$, where N shows the total number of ions in one cluster, which consists of identical ions. In our case this approximation is not valid, because the solid Al electron number density is so high that the wake field generated by a Si ion does not cover all or most of the other clustered ions within one cluster, as discussed above.

However, the tail of the wake field is rather long, as shown in Figs. 1 and 2. When two Si ions consisting of a small cluster move together in parallel to the moving direction, the wake field has an influence on the other ion behind it. Especially in our parameter range of the high-energy-density solid Al state and of the high speed of the Si, the wake field can cover Si ions just behind the forward-moving Si involved. Figures 3 presents the time evolution of six Si ions in one Si cluster at (a) $t = 0$, (b) 0.5 fs, (c) 1.0 fs, and (d) 1.5 fs. The Si cluster composed of six Si ions interacts with the solid Al. In each figure, the number besides each Si ion shows the identity number of each Si ion: For example, (1) in the term Si(1) shows the identity number for the Si. The Si cluster speed is $v_x = 0.221c$, and the six Si cluster structure is a regular octahedron with a side length of 5 Å: Therefore, the length between Si(1) and Si(2) is $5 \times \sqrt{2.0}$ Å. As presented above, the forward-moving Si(1) is caught and overtaken by Si(2), which is located just behind Si(1) in parallel. Each Si ion creates a wake field, and the electric field is localized in an elongated transversely limited area as shown in Fig. 2. Among the six Si ions consisting of the Si cluster, only Si(2) feels the wake field by Si(1). The other five Si ions dissipate their energy, as shown clearly in Fig. 3(d) and also in Fig. 3(b). Figure 4(a) presents the time sequence of the x position and Fig. 4(b) shows the history of the Si ion kinetic energy $(\gamma - 1)$ for Si(1) and Si(2). Each Si ion in one Si cluster creates a wake field, which is localized, and the kinetic energy of Si(1) is lost as an isolated ion is decelerated without the correlation as shown in Fig. 4(b). However, Si(2) is located just behind Si(1) (see Fig. 3), and feels the wake field from Si(1). The wake field from Si(1) is an acceleration field for Si(2), which also creates the wake field behind Si(2). The acceleration and deceleration fields are almost balanced on Si(2), though the deceleration field is slightly stronger so that Si(2) loses its energy slightly before the overtaking time of around $t =$ 0.57 fs in this example [see Fig. 4(a)]. After the overtaking time, Si(2) starts to lose its energy as Si(1) [see Fig. 4(b)]. When Si(2) approaches Si(1) as shown in Fig. 3(c), Si(1) and Si(2) interact with each other in the longitudinal and also in the transverse direction. In this case the transverse interaction between Si(1) and Si(2) becomes noticeable. Therefore, after Si(1) and Si(2) exchange their positions with each other as presented in Fig. 3(d), Si(1) and Si(2) separate mutually in the transverse direction. Initially, Si(1) and Si(2) are aligned longitudinally [see Fig. 3(a)], and at the close interaction time Si(1) and Si(2) are misaligned by the interaction [see Fig. 3(d)]. Therefore, after the first position exchange between Si(1) and Si(2), the next position exchange between Si(1) and Si(2) is not expected by the longitudinal misalignment.

The peculiar behavior of the Si ion discussed in this Rapid Communication arises in a short timescale τ of about a few fs or less. In the present case, the collisional frequency ν_{ie}

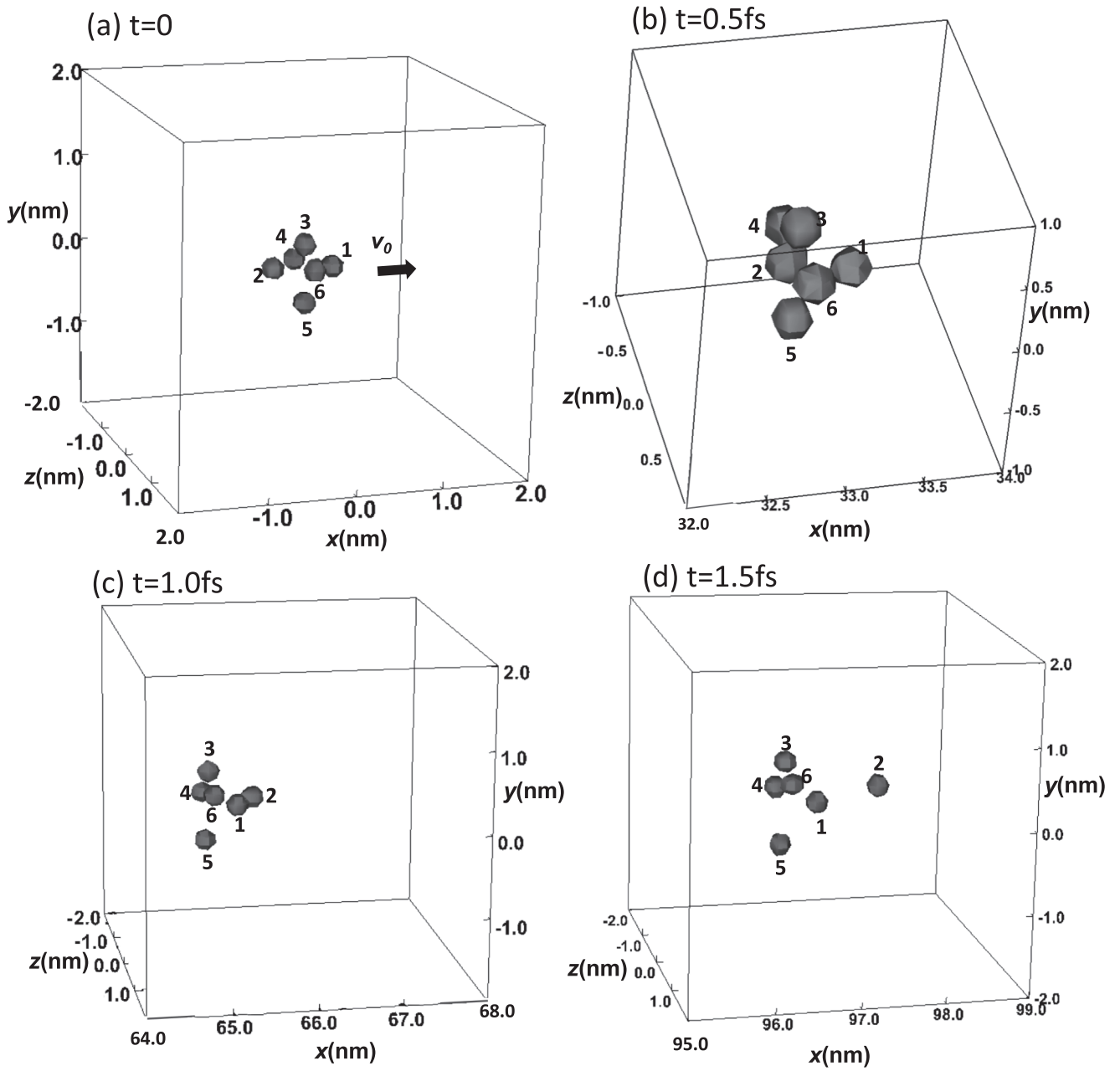

FIG. 3. A Si cluster, composed of six Si ions, interacts with the solid Al. The Si cluster speed is $v_x = 0.221c$. The six Si ions consists of a regular octahedron, and the distance between the adjacent two Si ions is 5 Å. The six Si ion positions at (a) $t = 0$, (b) 0.5 fs, (c) 1.0 fs, and (d) 1.5 fs.

between a Si ion moving with $0.221c$ and the electrons of the solid Al is much smaller than $1/\tau$. Therefore, the collective behavior of the high-density Al electrons, that is, the wake field, mainly contributes to the Si cluster interaction in the solid Al during τ. In addition, it should be pointed out that the overtaking behavior of the Si ions focused in this work may be difficult to be observed experimentally, because it is hard to distinguish one Si from another in one Si cluster. In addition, in the solid Al, the directional alignment control of one cluster is also difficult. The wake field is localized in space, and therefore, if the Si cluster in Fig. 3 rotates from its moving direction, Si(2) may not be covered by the Si(1) wake field. In this case, the Si ion overtaking behavior may not take place.

Figures 5 demonstrates the cluster alignment effect on the ion interaction with high-energy-density Al. In Fig. 5, three Si clusters, traveling in x with $0.221c$, interact with the solid Al at a temperature of 10 eV. Each cluster consists of two Si ions, and the distance between the two Si ions of each cluster is $5 \times \sqrt{2.0}$ Å. Cluster 2 is located in the middle of each figure, and has two Si ions in parallel to x. Cluster 1 is rotated by 45°, and cluster 3 by 90°. Figure 5(a) shows the initial state of the three clusters. Figure 5(b) shows that only Si(2b) catches up to Si(2a) at $t = 0.7$ fs. In Fig. 5(c), Si(2b) exchanges positions with Si(2a) at $t = 1.4$ fs. The wake field generated by each ion is localized transversely in the high-energy-density Al. The Si ions except for Si(2b) do not feel the wake field, and lose their

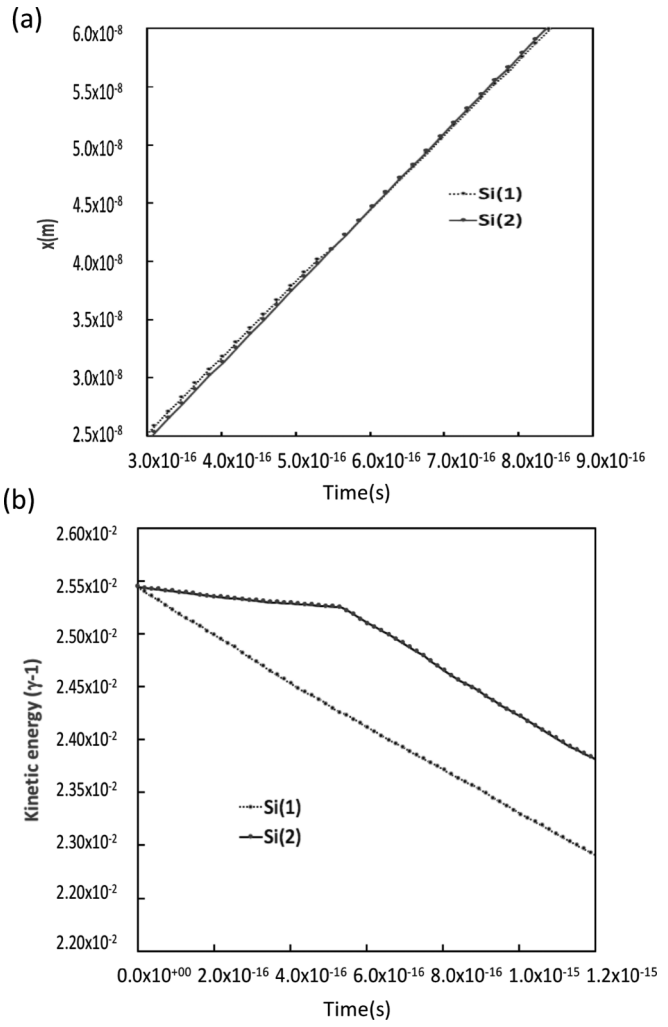

FIG. 4. (a) The history of the position in x, and (b) the kinetic energy history for Si(1) and Si(2) in one Si cluster, which is composed of six Si ions moving in the solid Al in the x direction. The forward-moving Si(1) dissipates its energy in the Al target, and the following Si(2) feels the acceleration wake field, generated by the forward-moving Si(1).

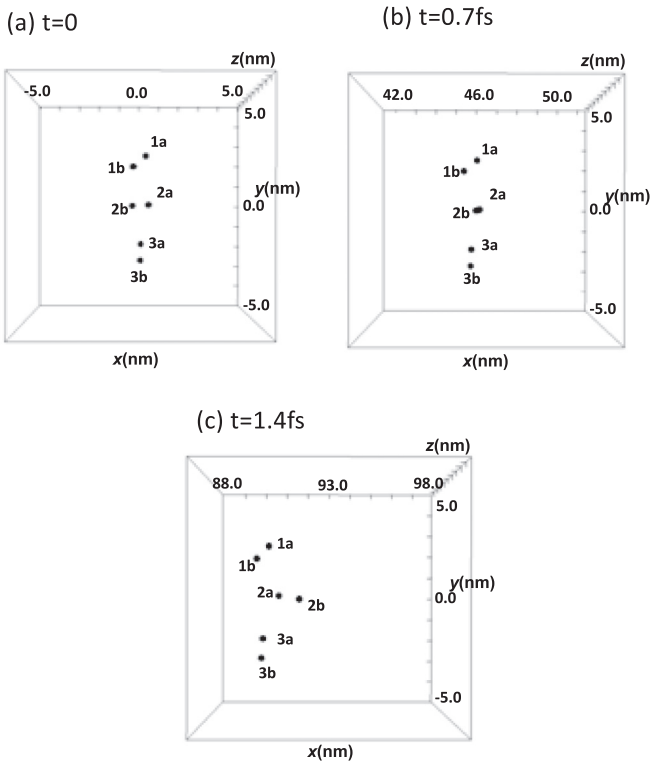

FIG. 5. Three Si clusters, traveling in x with $0.221c$, interact with the solid Al at a temperature of 10 eV. Each cluster consists of two Si ions. Cluster 2 is located in the middle of each figure, and has two Si ions in parallel. Cluster 1 is rotated by 45°, and cluster 3 by 90°. (a) The initial state of the three clusters. (b) Only the Si(2b) catches up to the Si(2a) at $t = 0.7$ fs, and (c) at $t = 1.4$ fs, Si(2b) exchanges positions with Si(2a). The wake field generated by each ion is localized transversely in the high-energy-density Al, and Si(1b), Si(3a), and Si(3b) do not feel the wake field. The Si ions, except for Si(2b), lose their energy, as an isolated ion loses its energy.

energy, as an isolated ion loses its energy. If the cluster-ion alignment is arranged well, as shown in cluster 2 in Fig. 5, and if one molecule composed of heterogeneous ions is used in experiments, the overtaking behavior would be observed experimentally.

In this Rapid Communication, we have presented peculiar ion motion in a cluster interacting with high-energy-density solid Al. In the context of ion beam inertial fusion, the target electron number density is high, and the ion or cluster speed is also large, $v_0/\sqrt{T_e/m_e} \gg 1$. Therefore, the wake field created by each ion in one cluster influences the ions just behind the ion concerned. In this extreme situation, the front ions lose their energy as an isolated ion loses its energy, and the ion just behind the forward-moving precursor ion in the cluster catches up to the forward ion and exchanges positions with that of the forward ion.

We thank K. Takayama, K. Horioka, T. Karino, M. Okamura, S. Kanesue, S. Ikeda, and J. Hasegawa for their discussions. This work was partly supported by Ministry of Education, Culture, Sports, Science and Technology (MEXT), Japan Society for the Promotion of Science (JSPS), Japan/U.S. Cooperation in Fusion Research and Development, and Center for Optical Research & Education (CORE) in Utsunomiya University. This work was also partly supported by the project ELITAS (CZ.02.1.01/0.0/0.0/16_013/0001793) and by the project High Field Initiative (CZ.02.1.01/0.0/0.0/15_003/0000449) both from European Regional Development Fund.

[1] Y.-N. Wang, H.-T. Qiu, and Z. L. Mišković, Phys. Rev. Lett. **85**, 1448 (2000).
[2] G. Wang, H. Yi, Y. Li, Y. Wang, D. Liu, F. Gao, W. Liu, J. Ren, X. Wang, Y. Zhao, and Y. Wang, Matter Radiat. Extremes **3**, 67 (2018).
[3] T. Ditmire *et al.*, Nature (London) **386**, 54 (1997).
[4] T. Ditmire *et al.*, Nature (London) **398**, 489 (1999).
[5] A. Brunelle *et al.*, Nucl. Instrum. Methods Phys. Res. B **125**, 207 (1997).

[6] K. Takayama, K. Koseki, K. Torikai, A. Tokuchi, E. Nakamura, Y. Arakida, Y. Shimosaki, M. Wake, T. Kouno, K. Horioka, S. Igarashi, T. Iwashita, A. Kawasaki, J.-I. Kishiro, M. Sakuda, H. Sato, M. Shiho, M. Shirakata, T. Sueno, T. Toyama, M. Watanabe, and I. Yamane, Phys. Rev. Lett. **94**, 144801 (2005).
[7] S. Kawata, T. Karino, and A. I. Ogoyski, Matter Radiat. Extremes **1**, 89 (2016).
[8] M. J. Clauser, Phys. Rev. Lett. **35**, 848 (1975).
[9] I. Hofmann, Matter Radiat. Extremes **3**, 1 (2018).
[10] N. A. Tahir *et al.*, Phys. Plasmas **4**, 796 (1996).
[11] C. Deutsch *et al.*, Fusion Technol. **31**, 1 (1997).
[12] G. Zwicknagel and C. Deutsch, Phys. Rev. E **56**, 970 (1997).
[13] A. Bret and C. Deutsch, J. Plasma Phys. **74**, 595 (2008).
[14] E. Nardi, Z. Zinamon, T. A. Tombrello, and N. M. Tanushev, Phys. Rev. A **66**, 013201 (2002).
[15] E. Nardi and Z. Zinamon, Phys. Rev. A **51**, R3407 (1995).
[16] D. Ben-Hamu *et al.*, Phys. Rev. A **56**, 4786 (1997).
[17] N. R. Arista, Nucl. Instrum. Methods Phys. Res. B **164–165**, 108 (2000).
[18] W. Brandt, A. Ratkowski, and R. H. Richie, Phys. Rev. Lett. **33**, 1325 (1974).
[19] D. S. Gemmell, J. Remillieux, J.-C. Poizat, M. J. Gaillard, R. E. Holland, and Z. Vager, Phys. Rev. Lett. **34**, 1420 (1975).
[20] K. Horioka, Matter Radiat. Extremes **3**, 12 (2018).
[21] Z. Vager and D. S. Gemmell, Phys. Rev. Lett. **37**, 1352 (1976).
[22] P. Chenevier, J. M. Dolique, and H. Perès, J. Plasma Phys. **10**, 185 (1973).
[23] C.-L. Wang, G. Joyce, and D. R. Nicholson, J. Plasma Phys. **25**, 225 (1981).
[24] P. M. Echenique, F. Flores, and R. H. Ritche, Solid State Phys. **43**, 229 (1990).
[25] S. Ichimaru, *Statistical Plasma Physics: Basic Principles*, 1st ed., Frontiers in Physics Vol. 1 (Westview Press, Colorado, 2004).
[26] N. R. Arista and W. Brandt, Phys. Rev. A **29**, 1471 (1984).
[27] G. Maynard and C. Deutsch, Phys. Rev. A **26**, 665 (1982).
[28] N. R. Arista and W. Brandt, Phys. Rev. A **23**, 1898 (1981).
[29] C. Ridgers *et al.*, J. Comput. Phys. **260**, 273 (2014).
[30] T. D. Arber *et al.*, Plasma Phys. Control. Fusion **57**, 113001 (2015).